Chapter 6

LiDAR for Geoscience Applications

Dong, Pinliang; Chen, Qi.
LiDAR Remote Sensing and Applications
CRC Press

6.1 INTRODUCTION

- The unique capability of LiDAR in providing highly accurate x, y, and z coordinates of ground points makes it an ideal data source for studying features on the Earth's solid surface.

- Six major fields of geoscience applications of LiDAR: (1) changes in geomorphic surfaces, including fundamental topographic signatures, alluvial fan (선상지) formative processes and debris flow deposits, volumetric changes of coastal dunes and beach erosion, changes in desert sand dunes, changes in glaciers/ice sheets and glacial sediment redistribution, and lava flow dynamics and rheology, (2) surface hydrology and flood models, (3) tectonic geomorphology, (4) lithological mapping, (5) rock mass structural analysis, and (6) natural hazards, such as landslides, debris flows, and earthquake damage

6.1 INTRODUCTION

- This chapter introduces LiDAR applications in the study of six major features/phenomena in geosciences: (1) Aeolian landforms (coastal dunes and desert dunes), (2) fluvial landforms (alluvial fans and terraces), (3) surface hydrology (watersheds and snow depth), (4) volcanic and impact landforms (volcanic cones and craters, lava flows, and impact craters), (5) tectonic landforms (linear and planar geomorphic markers), and (6) rocks and geologic structures.

6.2 AEOLIAN LANDFORMS

- Aeolian sand dunes are a major component of Aeolian landforms, and one of the most dynamic landforms on Earth and some other planets such as Mars and Venus and the moon Titan (of Saturn).

- Since 2000 there has been a shift in sand dune research focus from studying single dunes to studying dunes as complex systems.

- 2007). In addition to numerous field studies around the world, many other methods have been developed for sand dune studies, including cellular automaton models, numerical models, flume experiments, landscape-scale experiments, and remote sensing methods

6.2 AEOLIAN LANDFORMS

- In comparison with traditional remote sensing techniques, LiDAR has provided unprecedented datasets for sand dune studies, mostly in the form of high-resolution and high-accuracy digital elevation models (DEMs).

- Early LiDAR-based sand dune studies focused on morphometry and evolution of coastal dunes.

- Figure 6.1 shows perspective views of LiDAR point clouds collected on October 18, 2010, for two coastal dune fields (Vila Nova and Garopaba) in southern Brazil.

- Since 2010, several studies have been conducted for desert dunes.

- Baitis et al. (2014) used a LiDAR-derived DEM of a representative portion of WSDF (White Sands Dune Field to characterize dune-field parameters.

6.2 AEOLIAN LANDFORMS

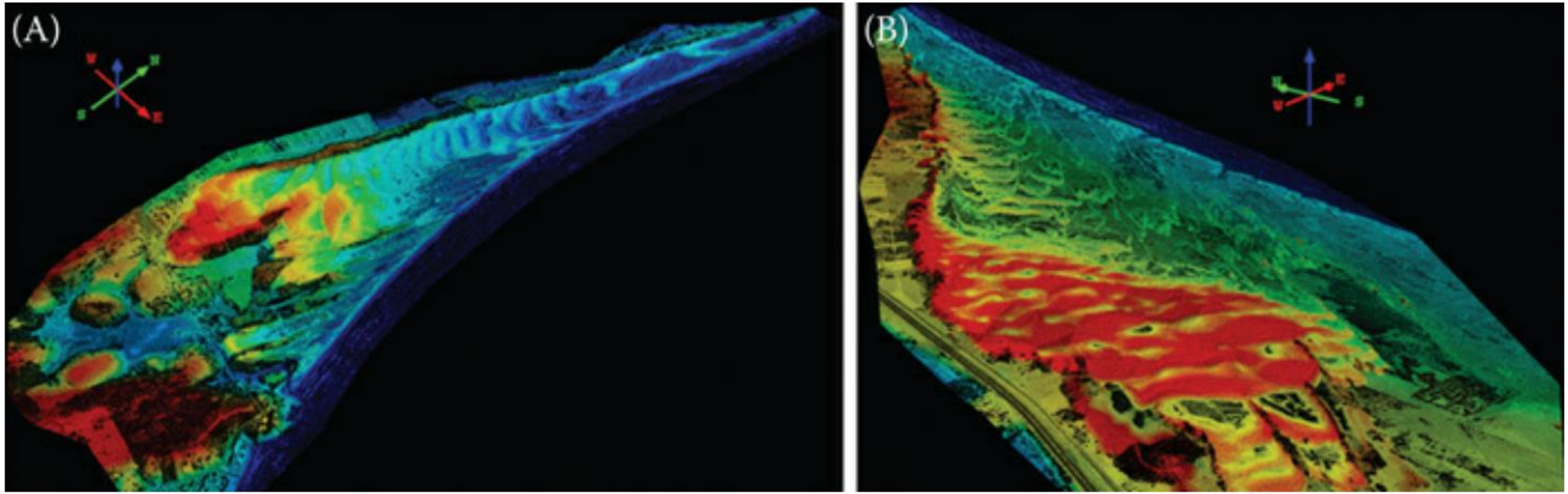

FIGURE 6.1 Perspective views of LiDAR point clouds collected on October 18, 2010 for two coastal dune fields—Vila Nova (A) and Garopaba (B) in southern Brazil.

6.2 AEOLIAN LANDFORMS

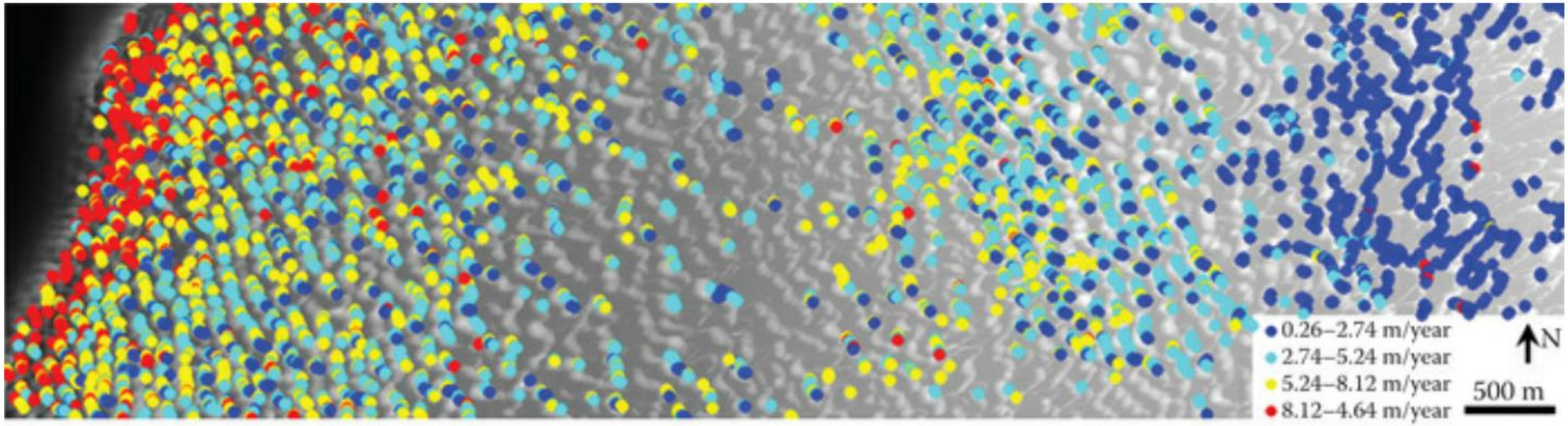

FIGURE 6.6 Sand dune migration rates of 5936 target points draped over LiDAR-derived DEM for June 6, 2010.

6.3 FLUVIAL LANDFORMS

- Alluvial fans have long been used as important records of quaternary climate and tectonics in arid and semiarid areas.

- Figure 6.9 shows 30-m resolution Landsat Thematic Mapper (TM) image, color composite of principal components of Landsat TM image bands, and a 1-m resolution hillshaded DEM derived from airborne LiDAR data for alluvial fans in Death Valley, California, USA.

- While optical images such as Landsat TM can provide spectral information of the alluvial fans, surface roughness is usually obtained from radar images. LiDAR provides a new data source for mapping surface roughness of alluvial fans using parameters such as slope, curvature, and aspect derived from high-resolution DEMs.

6.3 FLUVIAL LANDFORMS

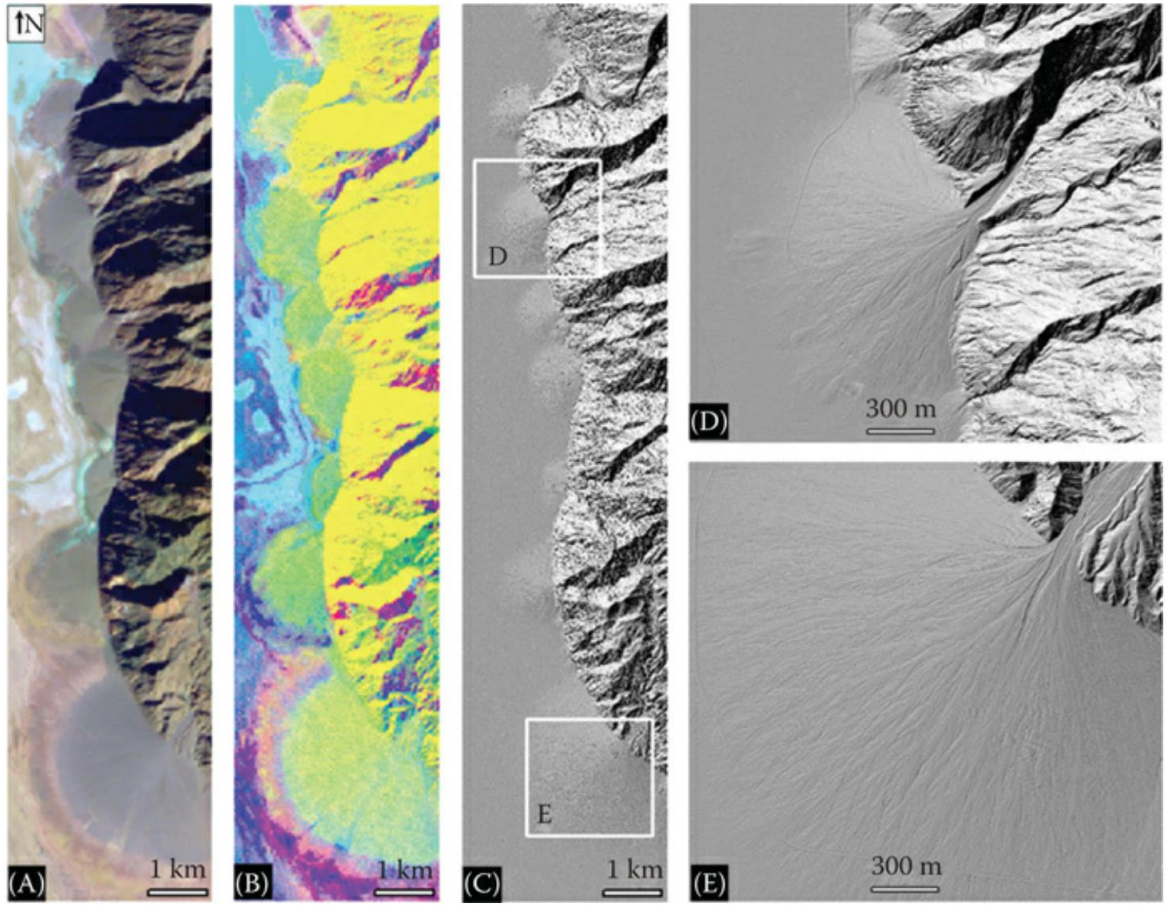

FIGURE 6.9 Landsat TM images and hillshaded DEM derived from LiDAR data for alluvial fans in Death Valley, California (USA). (A) Landsat TM image; (B) Color composite of principal components of Landsat TM bands; (C) Hillshaded DEM created from LiDAR data and (D) and (E) Sub-windows for two alluvial fans.

6.3 FLUVIAL LANDFORMS

- Terraces can be formed in different geologic and environmental settings. High-resolution and high-accuracy DEMs derived from LiDAR data can be very useful in studying terrace formation and abandonment.

- Figure 6.10 shows a LiDAR-derived DEM of a section of South Fork Eel River, CA, USA.

- Two profiles across the terraces and river bed are shown in Figure 6.11, which shows that LiDAR data can reveal terraces, as well as micro-topographic variations on the terraces.

6.3 FLUVIAL LANDFORMS

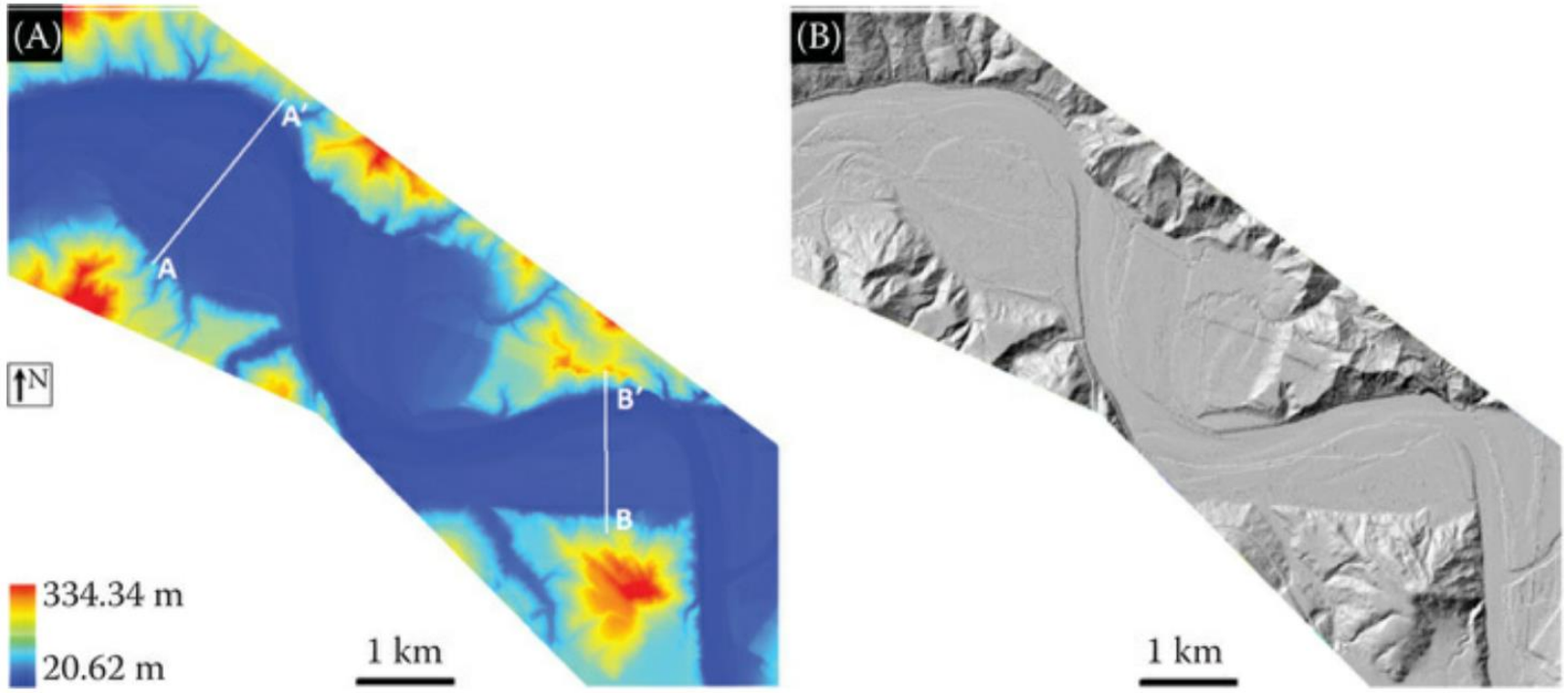

FIGURE 6.10 LiDAR-derived DEM of a section of South Fork Eel River, CA (USA). (A) 1-m resolution DEM; A-A′ and B-B′ are profile locations. Profiles are shown in Figure 6.11 and (B) hillshaded DEM.

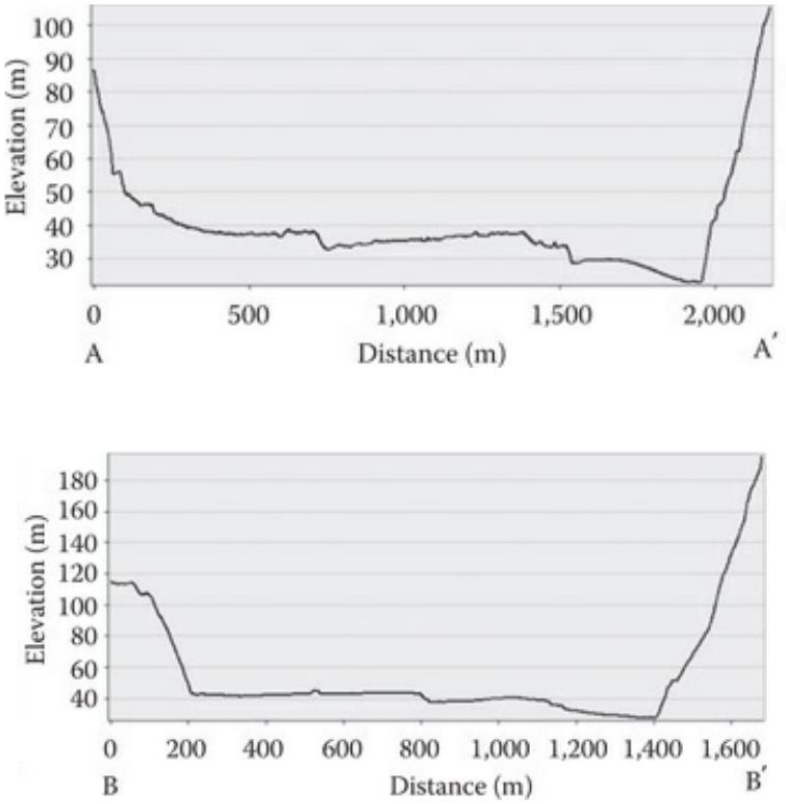

FIGURE 6.11 Topographic profiles derived from Figure 6.10A.

6.4 SURFACE HYDROLOGY

- Surface hydrology is closely related to precipitation, evaporation, river channels, watersheds, and human activities, among others. This section provides examples of LiDAR data for mapping watersheds and snow depth distribution.

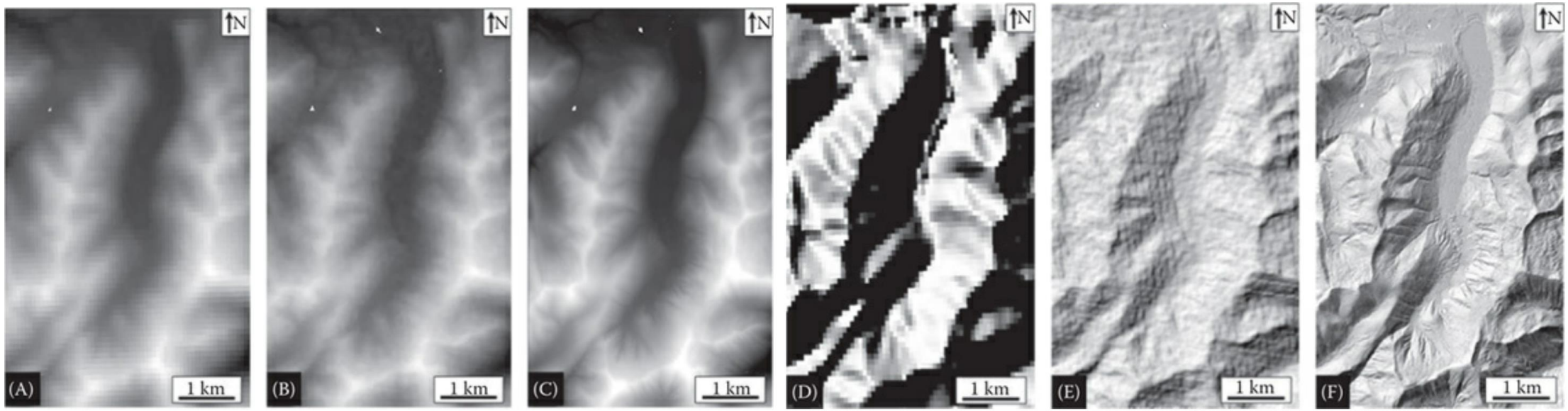

FIGURE 6.12 Comparison of DEMs derived from 90-m resolution SRTM (A and D), 30-m resolution ASTER GDEM (B and E), and 1-m resolution LiDAR-derived DEM (C and F) for a watershed in the Sawtooth National Forest, ID.

6.4 SURFACE HYDROLOGY

- The heterogeneous distribution of snow cover in mountain watersheds can be caused by the variability in meteorological, topographical, and vegetative controls, among other factors.

- The spatial distribution of snow depth can be obtained from LiDAR data collected in snow-on and snow-off conditions.

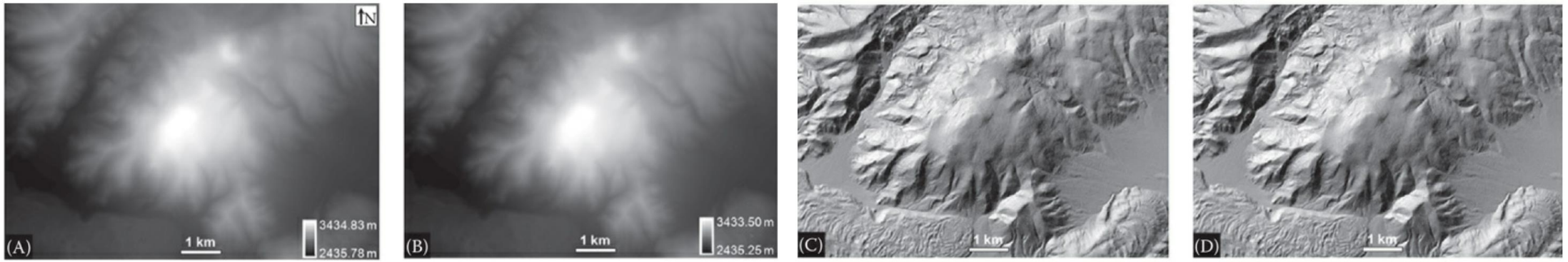

FIGURE 6.13 Original DEM and shaded DEM obtained from snow-on (A and C) and snow-off (B and D) LiDAR data collected in the upper Jerez river basin, NM (USA). Note the vertical coordinate system is NAVD88 (GEOID03) [EPSG: 5703].

6.4 SURFACE HYDROLOGY

- To further investigate the snow depth distribution, snow-on and snow-off topographic profiles are extracted from profile P–P′ (Figure 6.15).

- It can be seen from Figure 6.15 that west- and northwest-facing slopes have minimal snow depths, whereas east- and southeast-facing slopes have increased snow depth, especially near the hill ridge. It is believed that wind is a major causal factor for snow redistribution in this case,

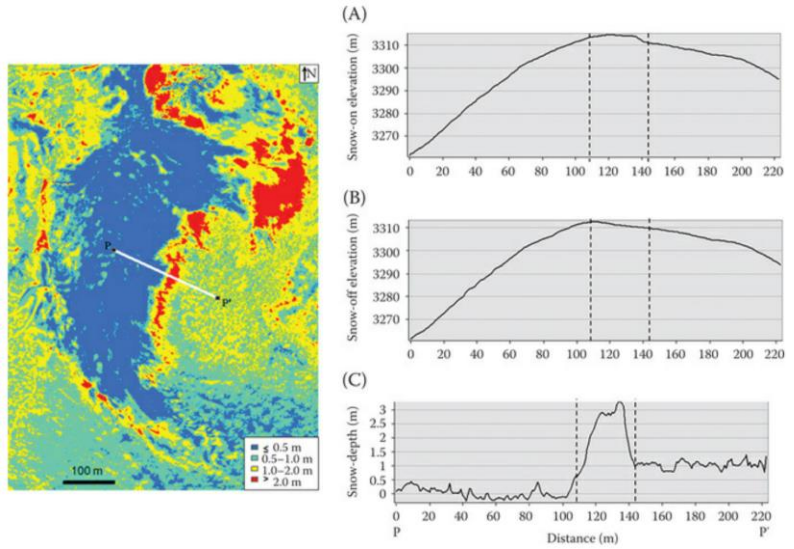

FIGURE 6.15 Classified snow depth map (left) and snow-on and snow-off topographic profiles (right). (A) Snow-on topographic profile; (B) snow-off topographic profile and (C) snow-depth profile derived from (A) and (B).

6.5 VOLCANIC AND IMPACT LANDFORMS

- Topography plays an important role in the emplacement of lava flows.
- High-resolution LiDAR data make it possible to investigate morphometric characteristics of lava flow.
- In this section, LiDAR data for several representative volcanic landforms are presented. Since impact craters and some volcanic craters have similar shapes, LiDAR for sample impact landforms is also presented.

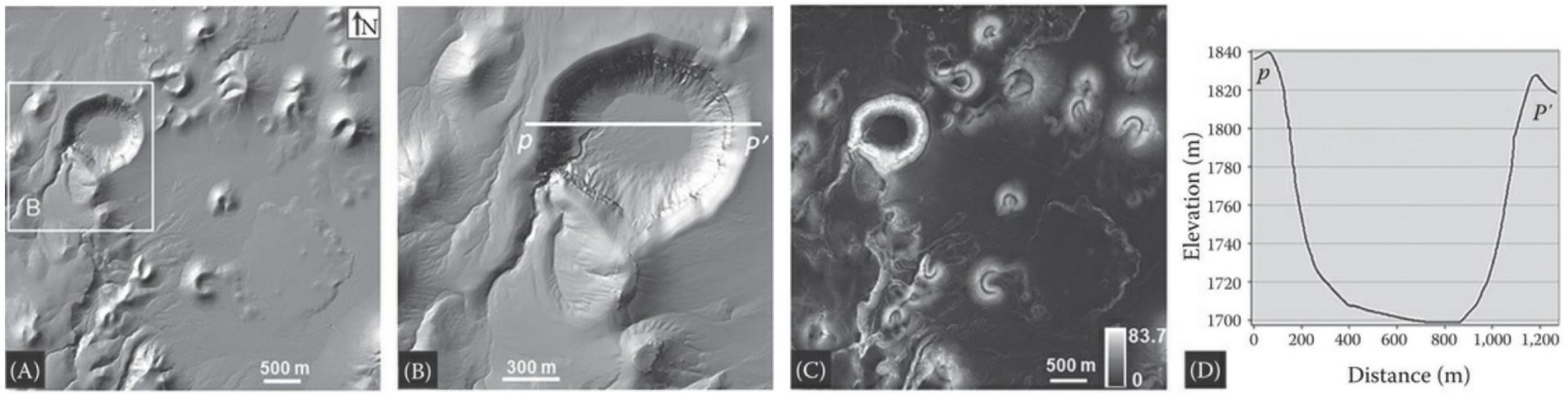

FIGURE 6.16 LiDAR-derived DEM products from part of the Lunar Crater volcanic field in east-central Nevada. (A) DEM; (B) A subarea extracted from (A); (C) Slope obtained from (A); (D) Profile extracted from pp′ in (B).

6.5 VOLCANIC AND IMPACT LANDFORMS

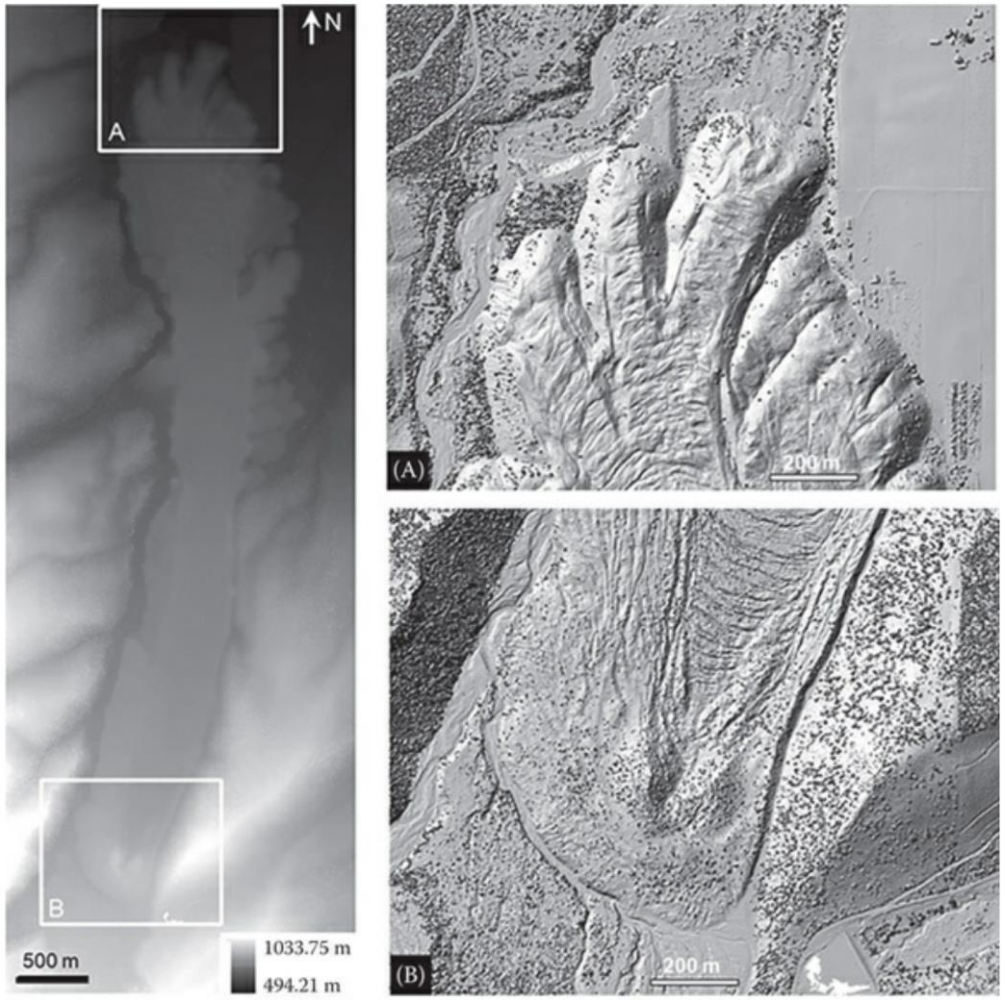

FIGURE 6.18 LiDAR data for Parkdale lava flow in Parkdale, OR (USA). Hillshaded DEMs are shown in (A) and (B). LiDAR data provided by the Oregon Department of Geology and Mineral Industries (DOGAMI) LiDAR Program.

6.5 VOLCANIC AND IMPACT LANDFORMS

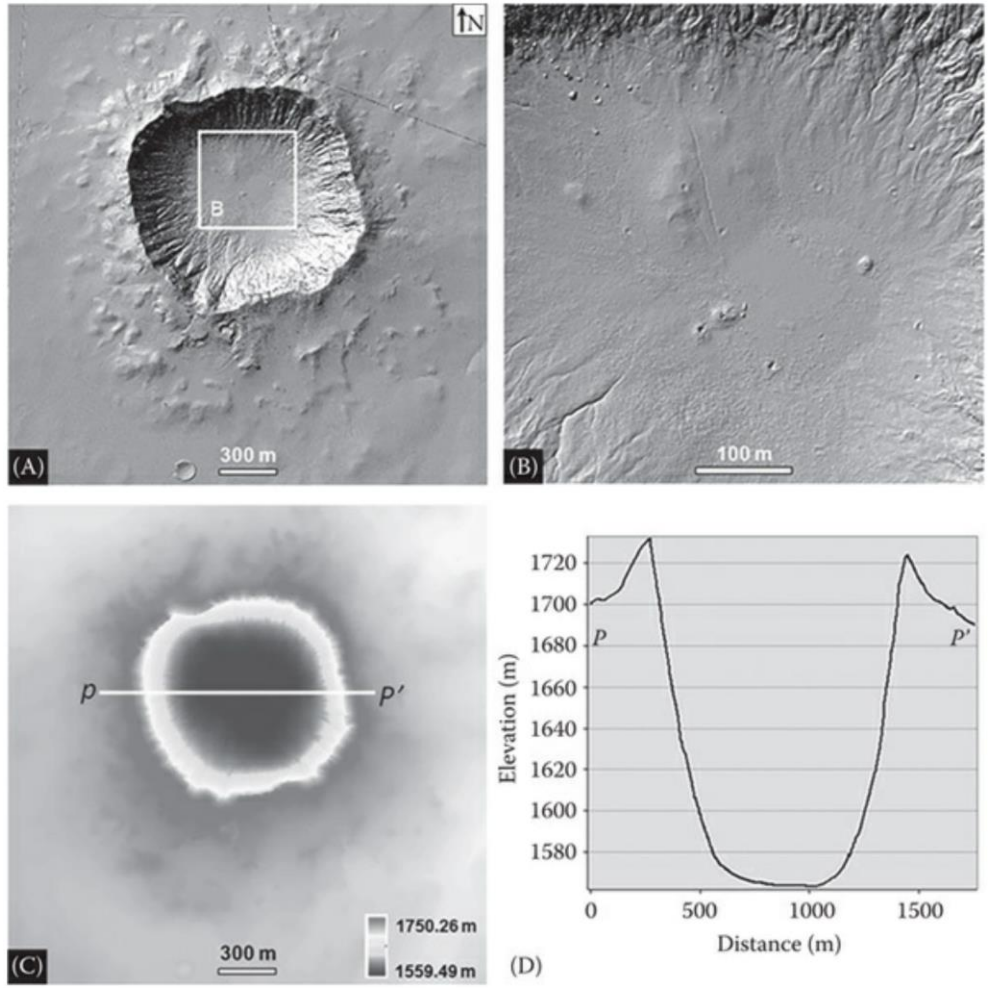

FIGURE 6.19 LiDAR-derived DEM products for Meteor Crater, AZ (USA). (A) and (B) Hillshaded DEMs; (C) DEM with colors for different elevations and (D) Topographic profile derived from P-P′ in Figure 6.19C.

6.6 TECTONIC LANDFORMS

- Numerous conceptual models of landscape evolution under tectonic and climate regimes have been proposed over the past century.

- To quantify the amount of tectonic deformation, identifiable geomorphic markers are needed to provide a reference frame.

- To calculate the rates of tectonic movement, two important parameters for geomorphic markers are needed: age and geometry.

- With increasing accuracy in dating geomorphic features, improvements in quantifying the geometry of geomorphic markers can produce more accurate rates of deformation.

- The last decade has seen wide applications of LiDAR in tectonic landform studies.

6.6 TECTONIC LANDFORMS

- With the use of LiDAR data for mapping recently active breaks in the Cholame segment of the south-central San Andreas Fault (SAF), a LiDAR-only approach is compared well with a combination of aerial photographic and field-based methods.

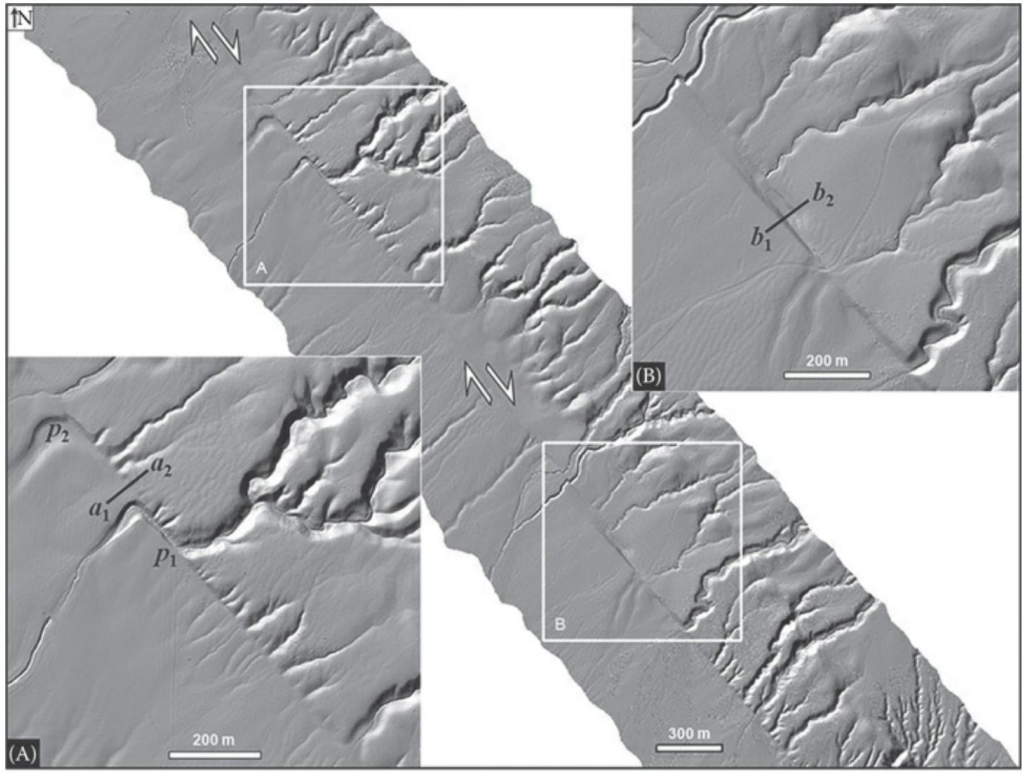

FIGURE 6.20 Offset channels in the south-central San Andreas Fault, CA (USA) shown in hillshaded DEM (1-m resolution) derived from LiDAR data. Two subareas are shown in (A) and (B).

6.6 TECTONIC LANDFORMS

FIGURE 6.21 Field photo of Wallace Creek taken near point p1 in Figure 6.20.

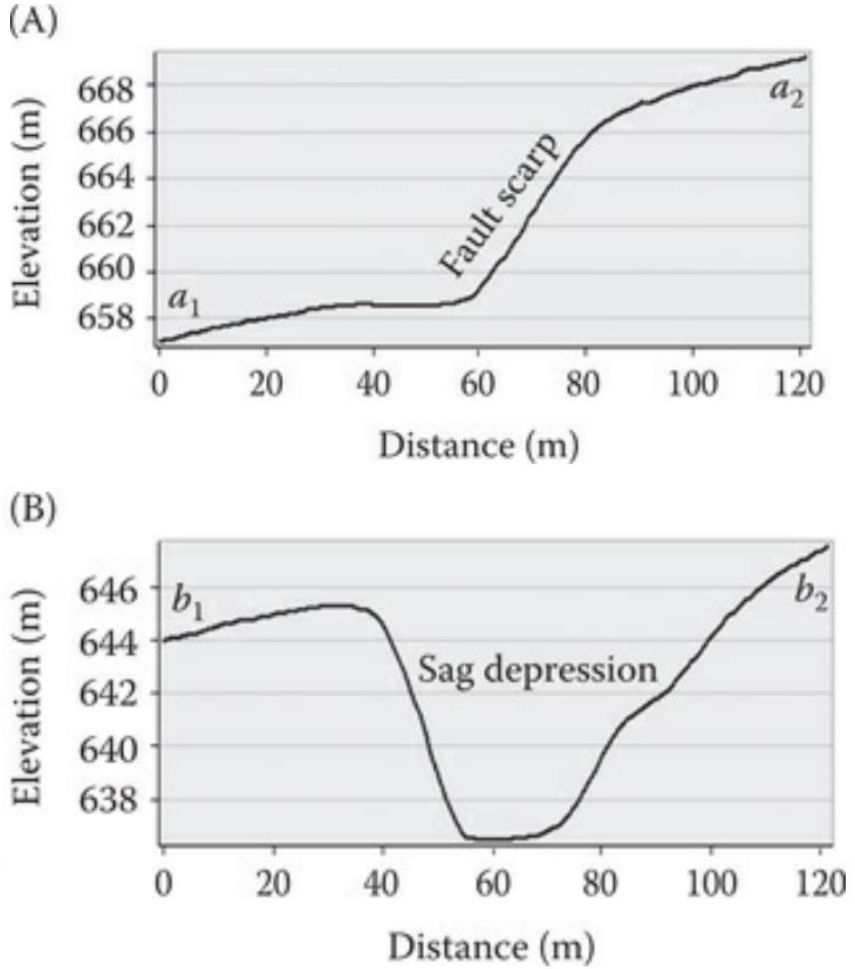

FIGURE 6.22 Topographic profiles extracted from a_1a_2 and b_1b_2 in Figure 6.20

6.7 LITHOLOGY AND GEOLOGIC STRUCTURES

- Compared with multispectral and hyperspectral image data that has been widely used in mapping rock units and geologic structures, the application of LiDAR data in lithological and structural mapping is relatively limited, mainly due to the lack of rich spectral information of LiDAR and relatively limited availability of LiDAR data.

- However, the capability of LiDAR in revealing topographic details, especially in areas of dense vegetation cover, can provide unique applications in mapping rock units and geologic structures.

- For lithological mapping in arid environments, integration of spectral information from optical images and texture information from radar images has proven to be effective in many studies. However in forested areas, textures from radar images usually reflect forest texture, not texture of the underlying ground surface.

6.7 LITHOLOGY AND GEOLOGIC STRUCTURES

- Grebby et al. (2010) used morphometric variables (including slope, curvature, and surface roughness) derived from a 4-m resolution LiDAR DEM to quantify the topographic characteristics of four major lithologies in the upper section of the Troodos Ophiolite, Cyprus, and produced a detailed lithological map that is more accurate than the best existing geological map in the area.

- Grebby et al. (2011) investigated the integration of airborne multispectral imagery and LiDAR-derived topographic data for lithological mapping in a vegetated section of the Troodos Ophiolite (Cyprus), and reported that LiDAR-derived topographic variables led to significant improvements of up to 22.5% in the overall mapping accuracy.

6.7 LITHOLOGY AND GEOLOGIC STRUCTURES

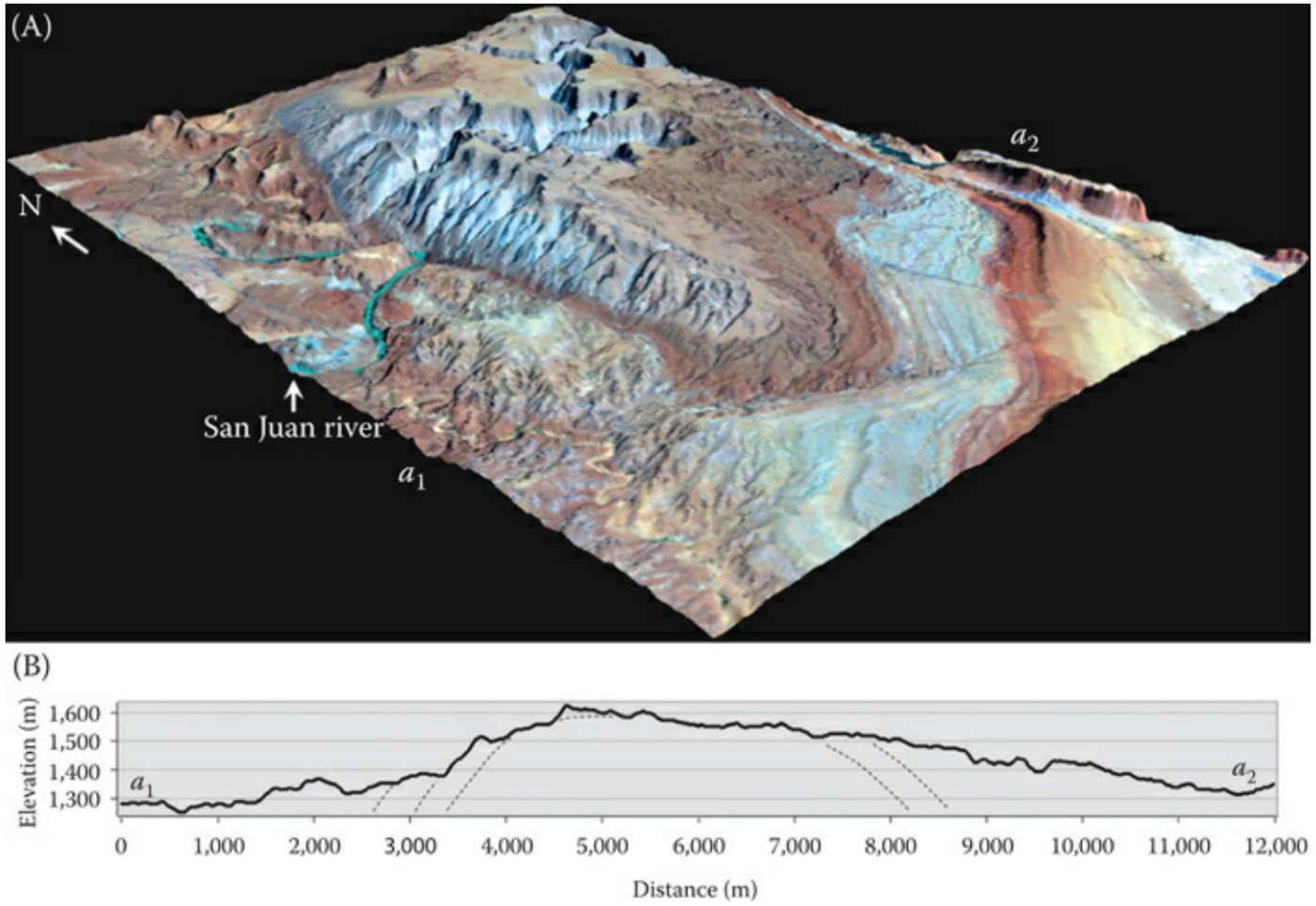

FIGURE 6.27 Raplee Ridge monocline in southwest Utah (USA). (A) Landsat TM 8 imagery [TM7 (R), TM3 (G), TM1 (B)] dragged over a vertically exaggerated (3×) ASTER GDEM digital elevation model and (B) Sketch profile from a1 to a2.

6.7 LITHOLOGY AND GEOLOGIC STRUCTURES

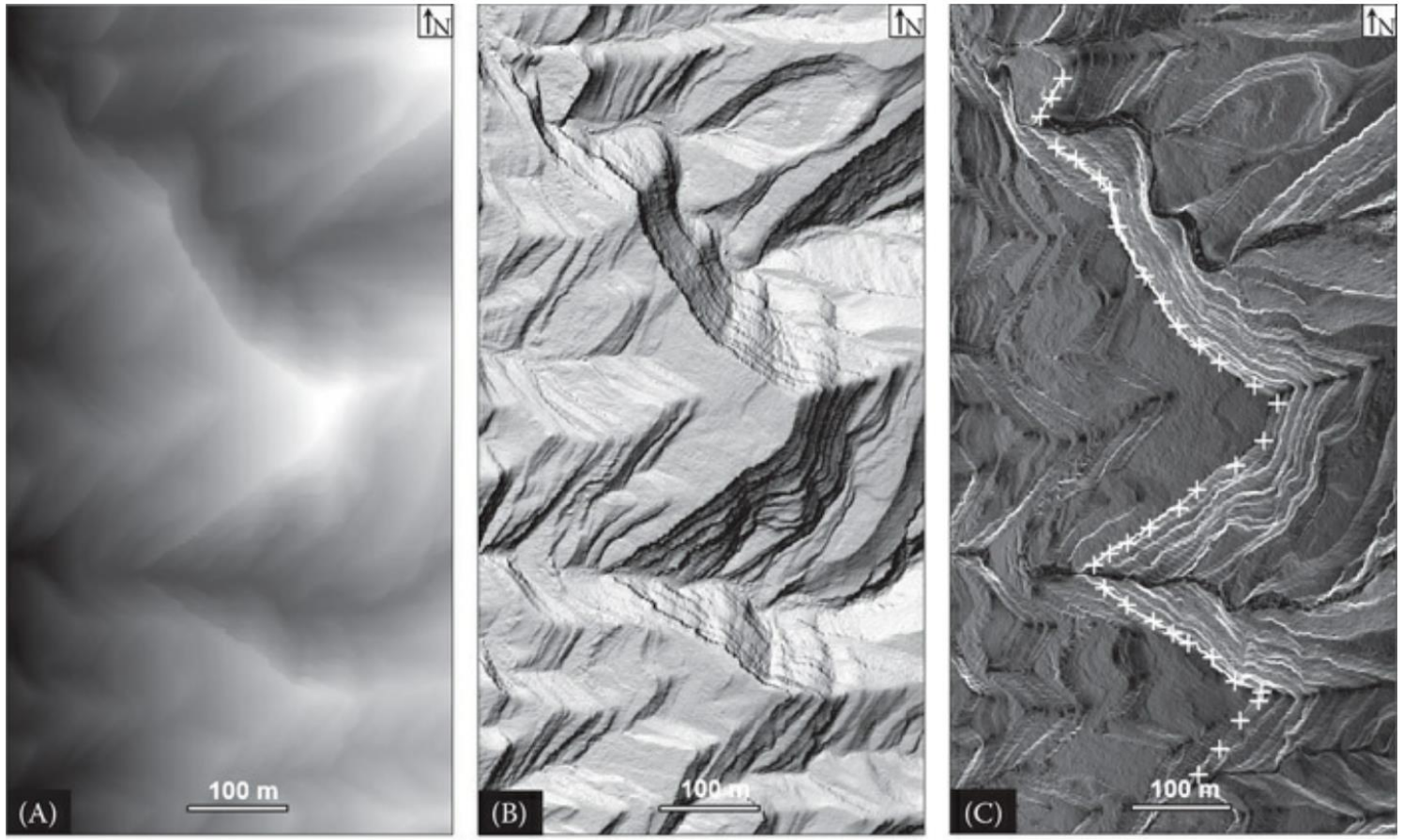

FIGURE 6.29 LiDAR-derived DEM products (1-m resolution) for box B in Figure 6.28A. (A) DEM; (B) hillshaded DEM and (C) slope raster created from DEM. White crosses in Figure 6.29C are sampling points along a rock layer

6.7 LITHOLOGY AND GEOLOGIC STRUCTURES

PROJECT 6.1: MEASURING SAND DUNE MIGRATION USING MULTI-TEMPORAL LiDAR DATA IN WHITE SANDS DUNE FIELD, NM, USA

PROJECT 6.2: DERIVING TREND SURFACES OF SIMPLE FOLDS USING LiDAR DATA IN RAPLEE RIDGE, UT, USA